Chapter 8
Improvements on Parametrized Joint Identification in Experimental Frequency-Based Substructuring

Jure Korbar, Domen Ocepek, and Gregor Čepon

Abstract How substructures interact at their interfaces plays a critical role in shaping the dynamic response of complex mechanical assemblies. Despite the localized nature of connections between substructures, their influence on the global response is significant and often complex to model. Variations in preload, temperature, vibration amplitude, etc. affect the dynamic properties of joints, limiting the effectiveness of analytical and numerical modeling approaches. To address these challenges, this work introduces a parametrization-based experimental joint identification framework, inspired by Lagrange multiplier frequency-based substructuring. This work proposes four distinct enhancements to the identification: the integration of sparse regression to promote model simplicity, the application of constraints based on rigid-body motion, a procedure for refining excitation directions, and an indirect parametrization strategy. These enhancements are applied to extract the joint's inertial, damping, and stiffness properties through a parametrized model. The approach is validated through both simulation and physical testing, demonstrating the added value of each modification and confirming the overall robustness and accuracy of the framework in capturing joint dynamics.

Keywords joint identification · regularization · virtual point transformation · impact excitation · dynamic substructuring

Introduction

Dynamic substructuring (DS) assembles component models by enforcing interface displacement compatibility and force equilibrium, while real connections rarely satisfy these ideal constraints, degrading predictions, especially with resilient mounts. To address non-ideal connections, two complementary strategies are common: transmission simulator (TS), where a representative substructure is mounted to replicate assembly interface conditions, and joint identification, which estimates the connection's dynamic properties for indirect coupling of substructures [2, 7].

Joint identification typically uses measured assembly FRFs and, when available, of the uncoupled components, to recover joint stiffness, damping, and mass properties, often via parametrized models [11, 9]. Inverse substructuring (IS) and frequency-based substructuring (FBS) have been applied to resilient interface connections; both benefit from virtual point transformation (VPT) to include rotational DoFs through interface deformation modes (IDMs), effectively mapping measured interface responses to six VP DoFs for substructuring and identification workflows [8, 3, 12]. Current applications emphasize bolted and resilient joints and explore robustness and data-driven identification within structural dynamics and structural health monitoring contexts [6, 1, 4].

This work focuses on a physical-domain joint parametrization using a twelve-DoF joint model and reformulates the Ren&Beards' method [9] in an LM-FBS inspired framework. Four modifications to the existing approaches are proposed: applying LASSO to promote sparsity, iteratively updating excitation directions within VPT, enforcing rank deficiency of joint stiffness and damping matrices via rigid-body mode constraints, and identifying the joint's dynamic stiffness first, followed by parametrization.

Jure Korbar · Domen Ocepek · Gregor Čepon
University of Ljubljana, Faculty of Mechanical Engineering
e-mail: jure.korbar@fs.uni-lj.si; domen.ocepek@fs.uni-lj.si; gregor.cepon@fs.uni-lj.si

© The Author(s), under exclusive license to River Publishers 2026

Kristin B. Zimmerman, PhD (eds.), *Dynamic Substructuring & Transfer Path Analysis, 2026, Vol. 4*, Conference Proceedings of the Society for Experimental Mechanics Series, https://doi.org/10.13052/rp-9788743814153

LM-FBS-Inspired Joint Parametrization

In cases where the joint inertial properties are negligible, the joint impedance matrix is not invertible due to the rank deficiency of stiffness and damping matrices[1], making the joint admittance matrix incalculable. Since LM-FBS decoupling produces an admittance matrix, this approach may not be appropriate to isolate the joint. Therefore, a joint identification approach which considers an impedance-based formulation of the joint model is advantageous.

For brevity, only two substructures A and B are considered, which are connected by a joint, denoted as J. To obtain the joint dynamics from the assembly AJB, the response, external excitation, and interface excitation DoFs, along with the uncoupled admittance matrix are respectively denoted as:

$$\boldsymbol{u} = \begin{bmatrix} \boldsymbol{u}^{\mathrm{A}} \\ \boldsymbol{u}^{\mathrm{B}} \end{bmatrix}, \quad \boldsymbol{f} = \begin{bmatrix} \boldsymbol{f}^{\mathrm{A}} \\ \boldsymbol{f}^{\mathrm{B}} \end{bmatrix}, \quad \boldsymbol{g} = \begin{bmatrix} \boldsymbol{g}^{\mathrm{A}} \\ \boldsymbol{g}^{\mathrm{B}} \end{bmatrix}, \quad \mathbf{Y}^{\mathrm{A|B}} = \begin{bmatrix} \mathbf{Y}^{\mathrm{A}} & \\ & \mathbf{Y}^{\mathrm{B}} \end{bmatrix}. \tag{1}$$

The response and excitation DoFs are related by the equation of motion:

$$\boldsymbol{u} = \mathbf{Y}^{\mathrm{A|B}} \left(\boldsymbol{f} + \boldsymbol{g} \right). \tag{2}$$

In the uncoupled state, the interface forces $\boldsymbol{g}$ acting on each of the substructures are zero. When coupled, the interface forces are subject to the joint dynamics, and are currently unknown. The joint response and excitation DoFs $\boldsymbol{u}^{\mathrm{J}}$ and $\boldsymbol{\lambda}$ are related by:

$$\mathbf{Z}^{\mathrm{J}} \boldsymbol{u}^{\mathrm{J}} = \boldsymbol{\lambda}, \tag{3}$$

where the joint impedance is denoted by $\mathbf{Z}^{\mathrm{J}}$. The interface forces $\boldsymbol{g}$ can be eliminated from Eq. (2) by establishing compatibility of interface and joint responses and equilibrium of interface forces and joint excitations:

$$\mathbf{B}_{\mathrm{u}}^{\mathrm{J}} \boldsymbol{u} = \boldsymbol{u}^{\mathrm{J}}, \tag{4a}$$

$$\boldsymbol{g} = -{\mathbf{B}_{\mathrm{f}}^{\mathrm{J}}}^{\top} \boldsymbol{\lambda}, \tag{4b}$$

leading to the following relation:

$$\left({\mathbf{Y}^{\mathrm{A|B}}}^{-1} + {\mathbf{B}_{\mathrm{f}}^{\mathrm{J}}}^{\top} \mathbf{Z}^{\mathrm{J}} \mathbf{B}_{\mathrm{u}}^{\mathrm{J}} \right) \boldsymbol{u} = \boldsymbol{f}, \tag{5}$$

where

$$\left({\mathbf{Y}^{\mathrm{A|B}}}^{-1} + {\mathbf{B}_{\mathrm{f}}^{\mathrm{J}}}^{\top} \mathbf{Z}^{\mathrm{J}} \mathbf{B}_{\mathrm{u}}^{\mathrm{J}} \right) = {\mathbf{Y}^{\mathrm{AJB}}}^{-1}. \tag{6}$$

Further rearranging leads to the initial joint identification equation:

$$\mathbf{Y}^{\mathrm{AJB}} {\mathbf{B}_{\mathrm{f}}^{\mathrm{J}}}^{\top} \mathbf{Z}^{\mathrm{J}} \mathbf{B}_{\mathrm{u}}^{\mathrm{J}} \mathbf{Y}^{\mathrm{A|B}} = \mathbf{Y}^{\mathrm{A|B}} - \mathbf{Y}^{\mathrm{AJB}}. \tag{7}$$

Eq. (7) is pre-multiplied by a weighing matrix $\mathbf{W}$ to mitigate the dominance of resonant peaks and relative difference in DoF responsiveness, as described in [9]. Vectorization of the weighed Eq. (7) facilitates joint parametrization:

$$\left(\left(\mathbf{B}_{\mathrm{u}}^{\mathrm{J}} \mathbf{Y}^{\mathrm{A|B}} \right)^{\top} \otimes \left(\mathbf{W} \mathbf{Y}^{\mathrm{AJB}} {\mathbf{B}_{\mathrm{f}}^{\mathrm{J}}}^{\top} \right) \right) \mathrm{vec}(\mathbf{Z}^{\mathrm{J}}) = \mathrm{vec} \left(\mathbf{W} \mathbf{Y}^{\mathrm{A|B}} - \mathbf{W} \mathbf{Y}^{\mathrm{AJB}} \right), \tag{8}$$

where $\mathrm{vec}(\star)$ denotes the column-major vectorization of $\star$. Parametrization of the joint is performed by expressing the impedance matrix in terms of the joint system matrices:

$$\mathbf{Z}^{\mathrm{J}} = \mathbf{P} \boldsymbol{\Omega}, \text{ where } \mathbf{P} \triangleq \begin{bmatrix} \mathbf{M}^{\mathrm{J}} & \mathbf{C}^{\mathrm{J}} & \mathbf{D}^{\mathrm{J}} & \mathbf{K}^{\mathrm{J}} \end{bmatrix} \text{ and } \boldsymbol{\Omega} \triangleq \begin{bmatrix} -\omega^2 \mathbf{I} & \mathrm{j}\omega \mathbf{I} & \mathrm{j} \mathbf{I} & \mathbf{I} \end{bmatrix}^{\top}, \tag{9}$$

leading to:

$$\mathrm{vec}(\mathbf{Z}^{\mathrm{J}}) = \left(\boldsymbol{\Omega}^{\top} \otimes \mathbf{I} \right) \mathrm{vec} \left(\mathbf{P} \right). \tag{10}$$

Additionally, since the system matrices should be symmetric to respect reciprocity, the vectorized system matrices can be expressed in terms of the unique system matrix terms:

$$\mathrm{vec}(\star) = \mathbf{L} \mathrm{vech}(\star), \tag{11}$$

[1] Only inertial forces oppose rigid body motion of a substructure with free boundary conditions, as rigid body motion translates to zero relative DoF displacements (and velocities). Therefore, stiffness and damping matrices of substructures with free boundary conditions must be rank-deficient.

where $\mathrm{vech}(\star)$ denotes the vectorization of the lower-triangular part of $\star$, regarded as half-vectorization. The set of unknown joint parameters $\boldsymbol{p}$ is defined as:

$$\boldsymbol{p} \triangleq \begin{bmatrix} \boldsymbol{m}^{\mathrm{J}} \\ \boldsymbol{c}^{\mathrm{J}} \\ \boldsymbol{d}^{\mathrm{J}} \\ \boldsymbol{k}^{\mathrm{J}} \end{bmatrix} \triangleq \begin{bmatrix} \mathrm{vech}(\mathbf{M}^{\mathrm{J}}) \\ \mathrm{vech}(\mathbf{C}^{\mathrm{J}}) \\ \mathrm{vech}(\mathbf{D}^{\mathrm{J}}) \\ \mathrm{vech}(\mathbf{K}^{\mathrm{J}}) \end{bmatrix}. \tag{12}$$

The parametrization is performed by combining the above equations written at frequencies of interest and further splitting into the real and imaginary components.[2] The final joint identification equation is written in a concise form:

$$\mathbf{A}\boldsymbol{p} = \boldsymbol{y}. \tag{13}$$

Indirect Joint Parametrization

One approach to improve the existing parametrization approach is to first identify the joint impedance matrix in the frequency domain by solving Eq. (7) for $\mathbf{Z}^{\mathrm{J}}$:

$$\mathbf{Z}^{\mathrm{J}} = \left(\mathbf{Y}^{\mathrm{AJB}}\mathbf{B}_{\mathrm{f}}^{\mathrm{J}\top}\right)^{+} \left(\mathbf{Y}^{\mathrm{A|B}} - \mathbf{Y}^{\mathrm{AJB}}\right) \left(\mathbf{B}_{\mathrm{u}}^{\mathrm{J}}\mathbf{Y}^{\mathrm{A|B}}\right)^{+}. \tag{14}$$

The initial joint impedance identification does not pose any restriction on weighting, expressing the impedance in terms of the joint system matrices, or accounting for reciprocity of system matrices.

Enforcing Rank Deficiency

Considering a massless joint, it is clear that the stiffness and damping matrices should be rank-deficient, as rigid-body motion consists of no relative DoF displacement, therefore, no force is required to perform rigid-body motion:

$$\mathbf{C}^{\mathrm{J}}\ddot{\boldsymbol{u}}_{\mathrm{RB}}^{\mathrm{J}} = \mathbf{0}, \quad \mathbf{D}^{\mathrm{J}}\boldsymbol{u}_{\mathrm{RB}}^{\mathrm{J}} = \mathbf{0}, \quad \mathbf{K}^{\mathrm{J}}\boldsymbol{u}_{\mathrm{RB}}^{\mathrm{J}} = \mathbf{0}. \tag{15}$$

By denoting the stacked rigid-body modes of the joint as $\mathbf{U}_{\mathrm{RB}}$ and taking symmetry of system matrices into account leads to a reduced set of stiffness and damping parameters $\tilde{\boldsymbol{c}}^{\mathrm{J}}$, $\tilde{\boldsymbol{d}}^{\mathrm{J}}$, and $\tilde{\boldsymbol{k}}^{\mathrm{J}}$ to be identified:

$$\boldsymbol{c}^{\mathrm{J}} = \mathbf{V}\tilde{\boldsymbol{c}}^{\mathrm{J}}, \quad \boldsymbol{d}^{\mathrm{J}} = \mathbf{V}\tilde{\boldsymbol{d}}^{\mathrm{J}}, \quad \boldsymbol{k}^{\mathrm{J}} = \mathbf{V}\tilde{\boldsymbol{k}}^{\mathrm{J}}, \quad \text{where} \quad \mathbf{V} \triangleq \mathrm{Null}\left(\left(\mathbf{U}_{\mathrm{RB}}^{\top} \otimes \mathbf{I}\right)\mathbf{L}\right). \tag{16}$$

Substituting the original parameters with the reduced set of parameters using Eq. (16) leads to rank deficient stiffness and damping matrices.

Sparse Regression

As least squares is prone to overfitting, sparse regression may allow to reduce overfitting by removing a subset of parameters identified as unimportant. In this work, LASSO [10] is chosen as the sparse regression approach, which is described by the following minimization problem:

$$\hat{\boldsymbol{p}} = \underset{\boldsymbol{p}}{\mathrm{argmin}} \left(\|\boldsymbol{y}^{\smile}\mathbf{A}\boldsymbol{p}\|_2^2 + \lambda\|\boldsymbol{p}\|_1\right), \tag{17}$$

where the hyperparameter λ determines the penalty strength. Increasing λ leads to sparser solutions, therefore, an appropriate value of λ should be chosen to strike the balance between joint model accuracy and sparsity. To reduce the effect of bias and also allow for applying RBM constraints, the LASSO solution $\hat{\boldsymbol{p}}$ is only used for parameter selection, which is followed by a least squares regression to solve for the values of the retained parameters. A more detailed description of how the selection is implemented to permit applying RBM constraints can be found in [5].

Excitation direction updating

Joint parametrization is based on the measured FRFs of the individual substructures and the assembly including the joint of interest. This work describes the joint using a twelve-DoF model with two nodes, i.e. six DoFs per node, which are obtained using VPT. As VPT is based on geometric relations, its accuracy is subject to precise positioning and orientation of response

[2] For a more detailed derivation, the interested reader is referred to [5].

and excitation DoFs. Excitation using an impact hammer is most common, which can lead to inaccurate excitation locations and directions. Assuming the main source of VPT inaccuracy lies in the excitation directions[3], this work introduces an iterative excitation direction updating algorithm to improve the VPT accuracy. The updating algorithm iteratively applies the VPT, enforces VP admittance reciprocity and calculates the excitation directions which reduce the discrepancy between the measured and projected (i.e. filtered) FRFs. The updating algorithm is depicted in Fig. 1.

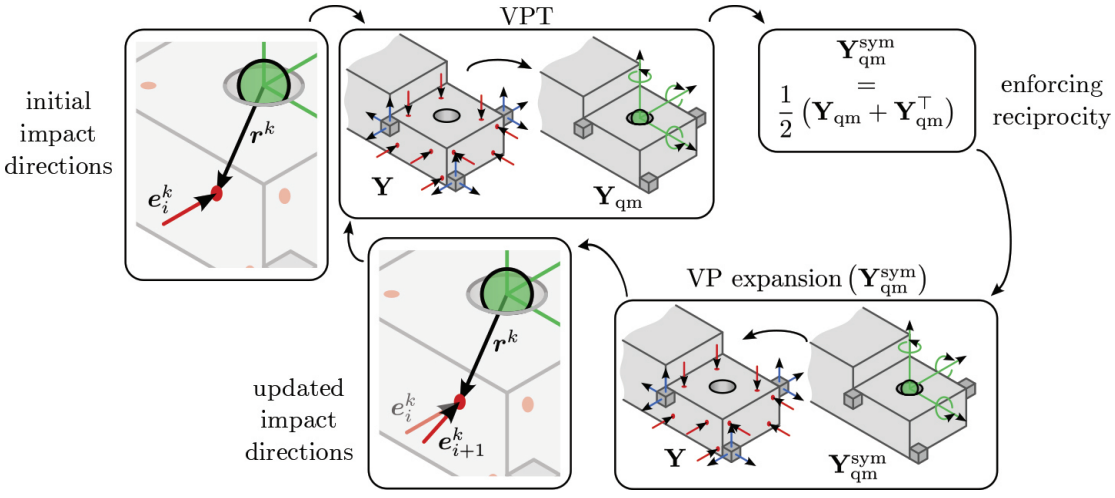

Fig. 1 Excitation direction updating algorithm.

Numerical study

The numerical study considers a CJC assembly (Fig. 2a) consisting of two cross substructures (C) and the rubber mount substructure (J), considered as the joint. The validity of the identified joint model is assessed in a cross validation procedure with the aim of estimating the dynamics of a separate AJB assembly (Fig. 2b), consisting of two substructures (A and B) connected by two rubber mounts.

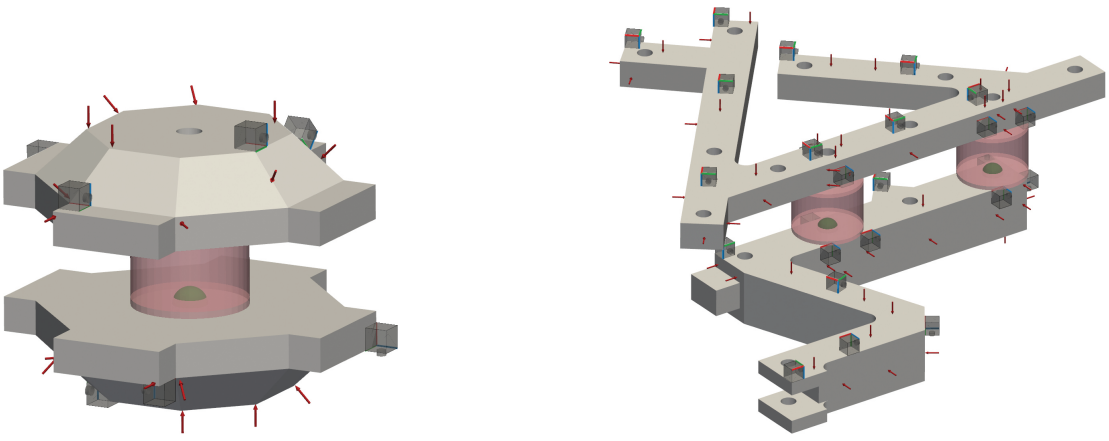

(a) (b)

Fig. 2 Numerical substructures: (a) CJC, (b) AJB.

[3] All terms in the IDM matrices are influenced by excitation directions, while only some are influenced by excitation locations, therefore, VPT is considered to be more sensitive to direction errors compared to location errors.

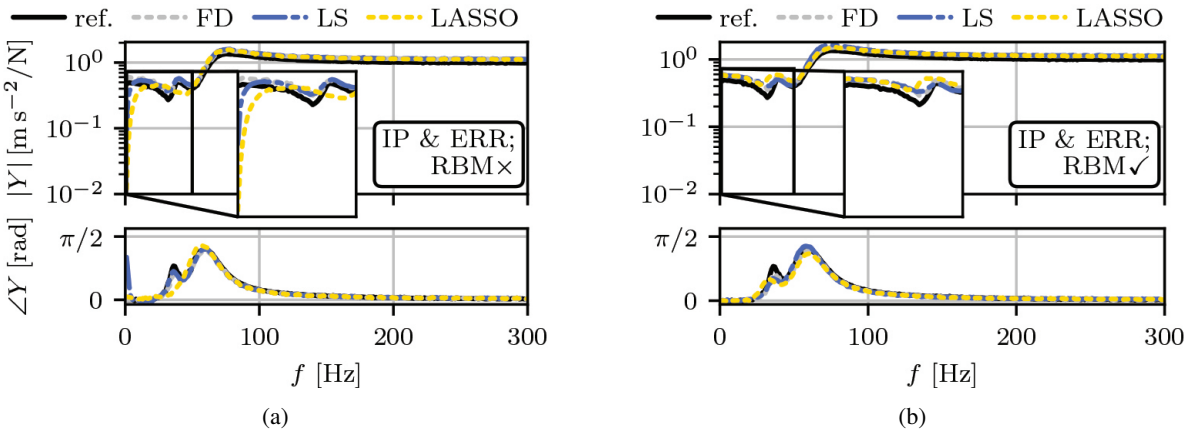

Fig. 3 CJC FRFs obtained using indirect parametrization and erroneous excitation directions: (a) no RBM considerations, (b) joint matrices constrained by RBMs.

The proposed modifications to joint parametrization are mutually independent and can be simultaneously applied, yielding 16 distinct parametrization approaches. Fig. 3 shows the improvement in estimated assembly dynamics by enforcing the rank deficiency of stiffness and damping matrices through the application of RBM constraints. This improvement was consistently observed, therefore, all remaining results shown in this work consider RBM constraints.

The following denotations are used to describe these modifications: DP and IP denote direct and indirect parametrization, RBM× and RBM✓ denote the non-applied and applied RBM constraints to enforce rank deficiency of stiffness and damping matrices, LS and LASSO denote least squares and LASSO, while ERR and UP denote the erroneous (original) and updated excitation directions. Results in Fig. 4 demonstrate that excitation direction updating leads to a more accurate estimation of assembly dynamics, regardless of the regression and parametrization approach. With DP, LASSO tends to slightly improve the estimation of assembly dynamics, while with IP, LASSO and LS solutions are comparable. Overall, IP improves the assembly dynamics estimation compared to DP.

In addition to the parametrization approaches, a frequency-dependent joint model was obtained from Eq. (14) (denoted as FD in Fig. 4), which was also used to estimate the assembly dynamics to compare the parametrized joint to the frequency dependent joint identification. Again, updating excitation directions significantly improved the estimation of assembly dynamics. The main advantage of a parametrized approach can be seen in the reduction of noise[4] in the estimation, as parametrization finds the optimal parameters for the chosen frequency range, while noise propagates through the frequency-dependent joint model.

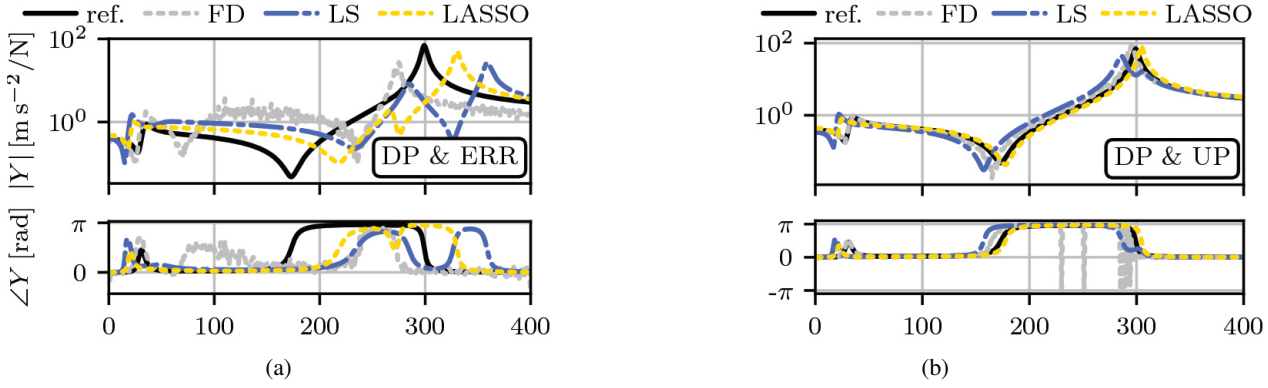

Fig. 4 *Continued*

[4]Noise was artificially added to the FRFs in the numerical study to better approximate real-world conditions.

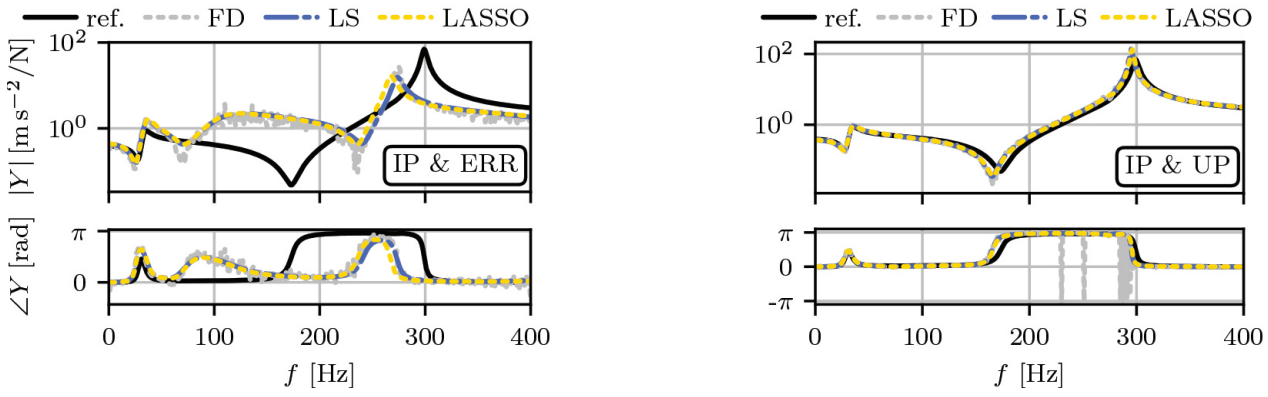

Fig. 4 Estimated AJB FRFs with RBM constraints: (a) DP without direction updating, (b) DP with direction updating, (a) IP without direction updating, (b) IP with direction updating.

Experimental study

Following the numerical study, an experimental study was also conducted to test the modified approaches in a real-world setting. Similar to the numerical study, two cross structrues were attached to a rubber mount to form a CJC assembly (Fig. 5a) to facilitate joint parametrization. The parametrized joint model was used to estimate the dynamics of AJB assembly (Fig. 5b), where substructures A and B were connected with two rubber mounts, as in the numerical study.

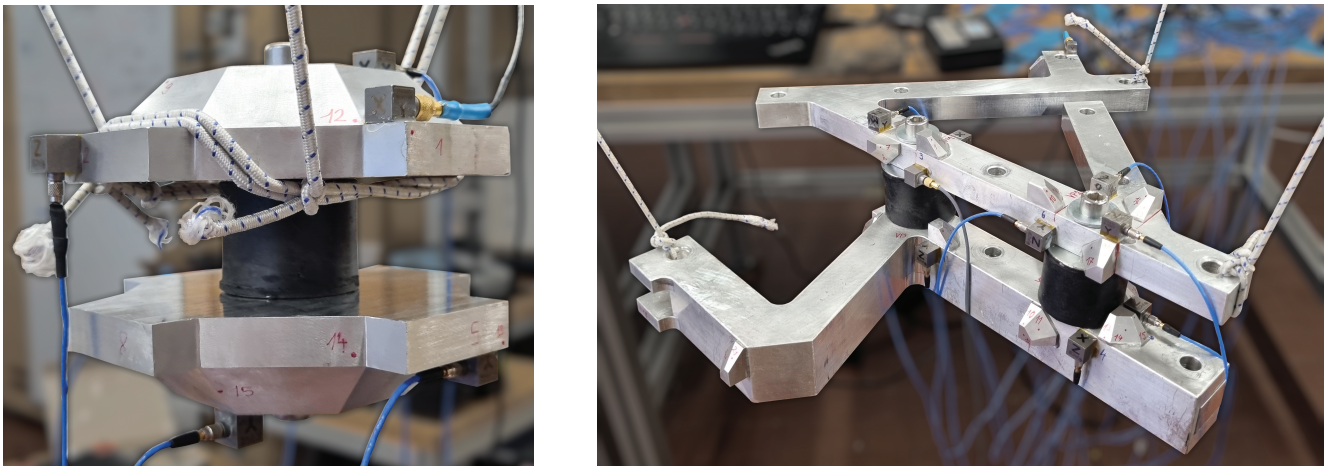

(a) (b)

Fig. 5 Experimental substructures: (a) CJC, (b) AJB.

The findings of the experimental study were fully aligned with the numerical study. Again, RBM constraints improved the estimation in the lower frequency range, therefore, only results of the remaining eight approaches are presented in Fig. 6. In line with the numerical study, updating excitation directions was seen to improve the estimated assembly dynamics, as well as replacing DP with IP, where LS and LASSO led to comparable results.

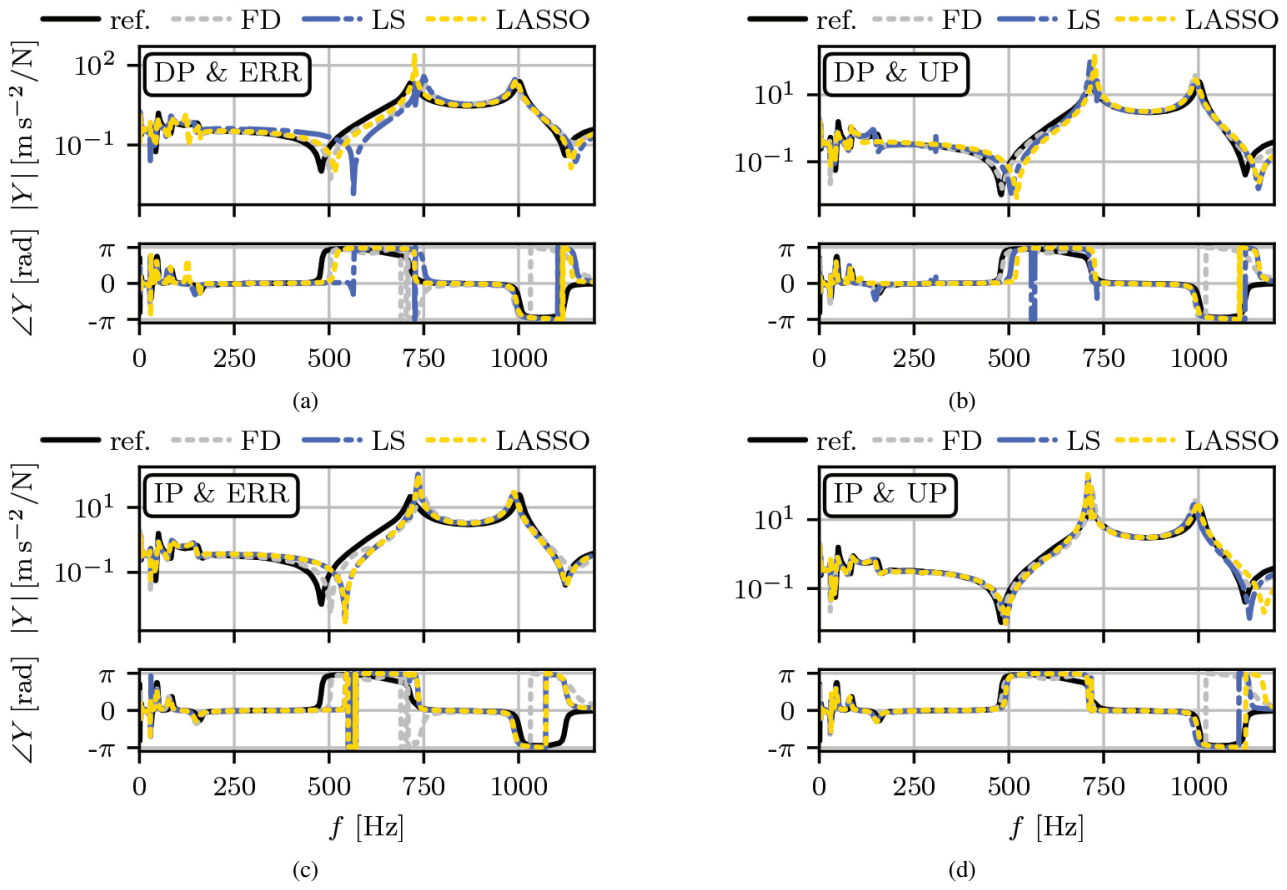

Fig. 6 Estimated AJB FRFs with RBM constraints: (a) DP without direction updating, (b) DP with direction updating, (c) IP without direction updating, (d) IP with direction updating.

Conclusion

This work explores four modifications to joint parametrization with the aim of improving the estimation of assembly dynamics using a parametrized joint model. These modifications can be applied independently, leading to 16 distinct parametrization approaches. Both numerical and experimental study confirmed that applying RBM constraints, updating excitation directions, and indirect parametrization are beneficial to the parametrization. Future research may focus on sparse regression approaches to further improve the parametrization procedure.

References

1. Marie Brons, Francesco Trainotti, and Daniel J. Rixen. *Estimating Linear Joint Stiffness and Damping Using a Frequency-Based Optimization Framework and the Emerging Concept of DyDis*, pages 37–42. 2025.
2. Dennis De Klerk, D. J. Rixen, and S. N. Voormeeren. General framework for dynamic substructuring: history, review and classification of techniques. *AIAA Journal*, 46(5):1169–1181, 2008.
3. M. Haeussler, S. W. B. Klaassen, and D. J. Rixen. Experimental twelve degree of freedom rubber isolator models for use in substructuring assemblies. *Journal of Sound and Vibration*, 474, 2020.
4. Jure Korbar, Domen Ocepek, Gregor Čepon, and Miha Boltežar. Training artificial neural networks using substructuring techniques: Application to joint identification. *Mechanical Systems and Signal Processing*, 198, 2023.
5. Jure Korbar, Domen Ocepek, Miha Pogačar, and Gregor Čepon. Towards an improved experimental joint identification in frequency-based substructuring. *Mechanical Systems and Signal Processing*, 238, 2025.
6. Michael Kreutz, Francesco Trainotti, Verena Gimpl, and Daniel J Rixen. On the robust experimental multi-degree-of-freedom identification of bolted joints using frequency-based substructuring. *Mechanical Systems and Signal Processing*, 203, 2023.
7. Randy L. Mayes. *Tutorial on experimental dynamic substructuring using the transmission simulator method*, pages 1–9. 2012.

8. J. W. R. Meggitt and A. T. Moorhouse. In-situ sub-structure decoupling of resiliently coupled assemblies. *Mechanical Systems and Signal Processing*, 117:723–737, 2019.
9. Y. Ren and C. F. Beards. Identification of joint properties of a structure using FRF data. *Journal of Sound and Vibration*, 186(4):567–587, 1995.
10. Robert Tibshirani. Regression Shrinkage and Selection via the Lasso. *Journal of the Royal Statistical Society: Series B (Methodological)*, 58(1):267–288, 1996.
11. J.-S. Tsai and Y.-F. Chou. The identification of dynamic characteristics of a single bolt joint. *Journal of Sound and Vibration*, 125(3):487–502, 1988.
12. Maarten van der Seijs, Daniël van den Bosch, D. J. Rixen, and Dennis de Klerk. An improved methodology for the virtual point transformation of measured frequency response functions in dynamic substructuring. *COMPDYN*, 2013.